ADVANCES IN MATERIALS SCIENCE, Vol. 24, No. 2 (80), June 2024

DOI: 10.2478/adms-2024-0010

Abdelghani Baltach[1,2], Foudil Khelil[2], Abdelkader Djebli[2], Ali Benhamena[2], Mohamed Ikhlef Chaouch[2]*, Mostefa Bendouba [2]

[1]*Department of Mechanical Engineering, University of Tiaret, Algeria*
[2]*Laboratory LPQ3M, BP763,University of Mascara, Mascara 29000, Algeria*

* *ikhlef.mohamed@univ-mascara.dz*

NUMERICAL INVESTIGATION OF INDENTATION-INDUCED RESIDUAL STRESSES AND THEIR EFFECT ON J-INTEGRAL AND CRACK PROPAGATION

ABSTRACT

This work presents an analysis of the effect of ball indentation on fatigue crack growth. The main objective is to assess the effectiveness of indentation, particularly its influence on the J-integral, as a fracture criterion governing fracture toughness. Using the finite element method in Abaqus 6.14, we analyzed the residual stresses induced by indentation at different positions along the predicted line of crack propagation and calculated the J-integral. The results highlight that indentation at the crack tip position significantly reduces the J-integral compared to non-indented structures, demonstrating its potential to extend the lifespan of cracked components by delaying crack propagation. The findings underscore the practical application of ball indentation as a viable technique to retard crack growth, contributing to the longevity of cracked components and, consequently, structural integrity. This analysis revealed a crack propagation retardation gain of up to 56%.

Keywords: *Residual stress; FEM; Indentation; J-integral; Crack growth*

INTRODUCTION

The historical development of indentation techniques, from Brinell's pioneering work in the 19th century [1–4] to modern methods such as nanoindentation and Instrumented Indentation Testing (IIT), underscores their significance in materials science [5–7]. These techniques find wide-ranging applications in industries, including material characterization, quality control, and fatigue and fracture resistance research [8–11].

In the context of fatigue resistance, controlled indentations strategically induce plastic deformation, creating compressive residual stresses around the indentation site [12–14]. These residual stresses act as a barrier against crack propagation, thereby enhancing the material's fatigue resistance. Industries, particularly those in aerospace and automotive sectors, leverage indentation to optimize material fatigue resistance, ensuring the longevity and safety of structural elements subjected to cyclic loading [15].

Finite Element Analysis (FEA) emerges as a crucial computational tool to analyze the interplay between indentation and fatigue crack retardation [16]. FEA allows for detailed modeling of indentation effects on metals, including the introduction of residual stresses and

Received: 2023.12.13; Received in revised form: 2024.02.24; Accepted: 2024.03.09

their impact on crack initiation and propagation. Moreover, the quantitative analysis of stress intensity factors (SIFs) at the crack tip aids in predicting crack growth behavior under various loading conditions [17,18].

Experimental studies explore the influence of applied force and residual stresses induced by indentation on crack propagation [19–21]. By systematically varying these parameters, researchers gain valuable insights into crack growth behavior under different loading conditions. These experiments involve subjecting materials to controlled indentation processes while monitoring crack initiation and propagation using advanced techniques such as optical microscopy, scanning electron microscopy (SEM), or acoustic emission response [13,22–24]. Through meticulous analysis of the resulting data, researchers quantify key parameters such as crack growth rates, lengths, and residual stress distributions near the indentation site.

In addition to indentation method, other techniques are employed for introducing residual stresses, such as the cold expansion method [25–27]. Subsequent studies aimed to optimize compression stresses around a fastener hole by analyzing the effect of plate thickness [26] and the taper angle of the pin [27].

Building upon previous research, the current work focuses on analyzing the effect of indentation and its position on the distribution of compressive residual stresses and the calculation of the J-integral using the finite element method. The obtained J-integral values for non-indented and indented cracked plate were then used to calculate the fracture crack growth rate using Forman empirical expression.

PROCESS AND GEOMETRIC MODEL

The indentation process is performed on plate containing fatigue cracks. A spherical indenter (ball) is used to create an impression at the front of the crack, as shown in Fig.1 and Fig.2. Subsequently, a uniaxial tensile load was applied to the indented plates to assess the influence of this impression on the generated residual stresses. In order to gain a better understanding of this process, the impression is applied at three positions along the crack propagation line (Fig.2a). This analysis allows us to determine the optimal impact of this technique on the induced compressive residual stresses and consequently, its effect on the crack propagation. This can be predicted by the J-integral calculation around the crack tip.

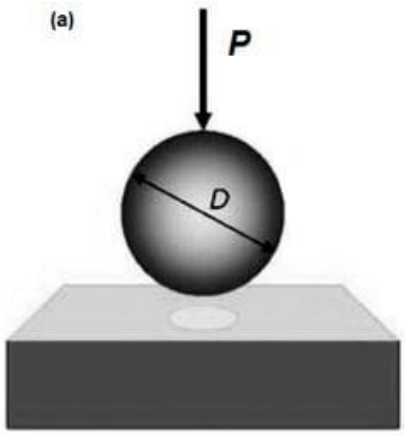

Fig. 1. Indentation process

A rectangular plate made with aluminum 7075-T6 alloy with a thickness of 3.175mm containing a lateral crack of length a = 5 mm is modeled. A spherical indenter with a radius R = 1mm is used to achieve the indentation process. The geometric models and dimensions of the cracked plate and the ball are given in Fig.2a and Fig.2b, respectively.

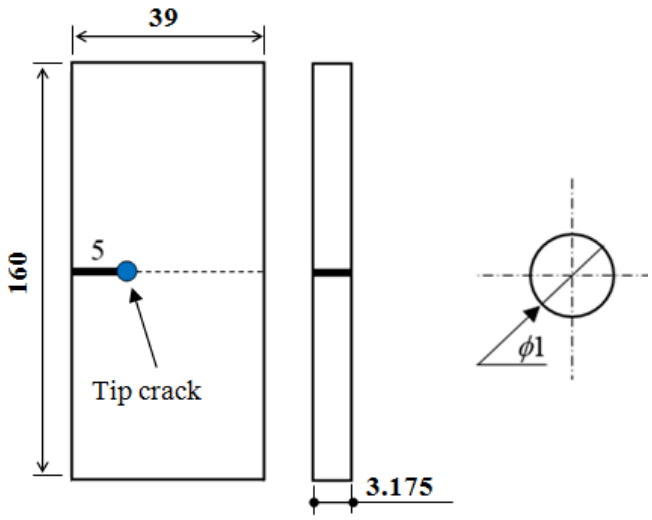

Fig. 2. Geometric model: a) Plate with edge crack; b) Spherical indenter (scale is magnified, dimensions in mm)

FINITE ELEMENT MODEL

A 3D finite element analysis was conducted using the Abaqus 6.14 software to calculate the residual stress field and resulting J-integral around the crack. To address the singularity at the crack front, the mesh underwent refinement to prevent degeneration of the results. Linear, fully integrated brick C3D8R elements were utilized to discretize the model. Beyond the singularity region (away from the crack front), the mesh density was gradually reduced using the same element type (Fig. 3). The interaction between the spherical indenter and the plate was modeled using surface-to-surface contact, with a friction coefficient of 0.1 applied between the ball and the cracked plate surfaces. Details regarding the size of the finite element model, including the number of nodes and elements, are provided in Table 1.

Table1. *Size of the finite element model*

Parts	Element Size	Number of elements	Number of nodes	Element Type
Cracked Plate	0.09 to 19	5920	7780	Linear Tetrahedral (C3D8R)

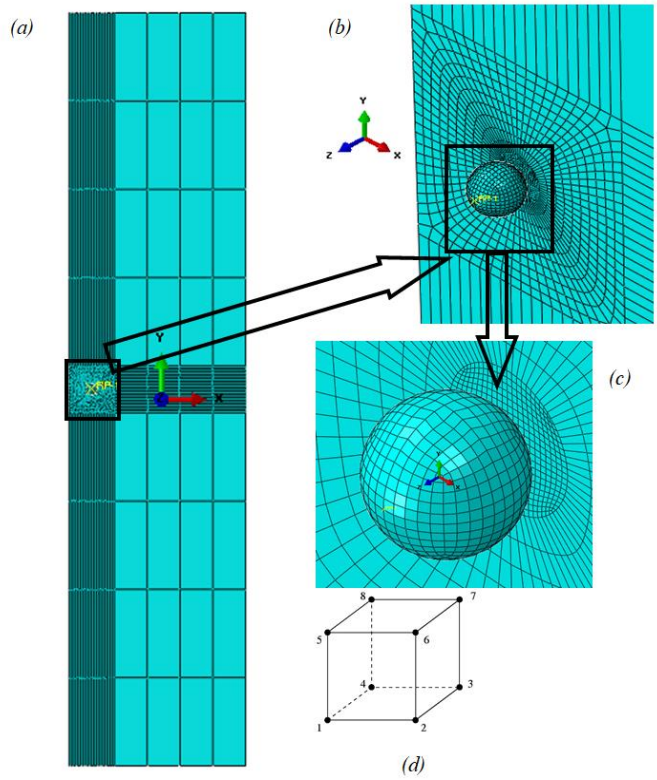

Fig. 3. Finite Element Model; (a) Typical mesh of the indented plate; (b) Mesh around the crack tip; (c) Mesh at the crack tip region; (d) C3D8R element type

Mechanical properties

The plate material selected for this analysis is Aluminum 7075-T6, known for its elastoplastic behavior. This material is commonly utilized in the aerospace industry due to its favorable mechanical properties. Additionally, we modeled the indenter using grade En 24 steel, which exhibits linear elastic behavior with high elastic modulus. The 7075-T6 Aluminum alloy was chosen based on its widespread use and compatibility with aerospace applications. The mechanical properties of the materials used in this study are presented in Table 2 [26].

Table 2. *Mechanical properties of the used materials [26]*

Material	Young's Modulus (GPa)	Poisson's Ratio	Yield Strength (MPa)
Aluminium 7075-T6	72	0.33	500
Steel En 24	210	0.3	-

Loading and Boundary conditions

To simulate the indentation process and assess the impact of resulting residual stresses, the calculation procedure will be carried out in two sequential steps.

In the first step, the plate undergoes indentation at the crack tip. The underside of the plate is clamped to ensure that nodes remain fixed in the X, Y, and Z directions, as illustrated in Fig. 4.a. Additionally, a displacement of 0.1 mm in the Z direction is applied to the spherical indenter, enabling it to penetrate the plate at the designated position before returning to its initial position (Fig. 4.b).

Subsequently, the second step involves clamping the inferior border edge of the plate and applying tensile stress in the other border in the Y direction, as illustrated in Fig. 4.c.

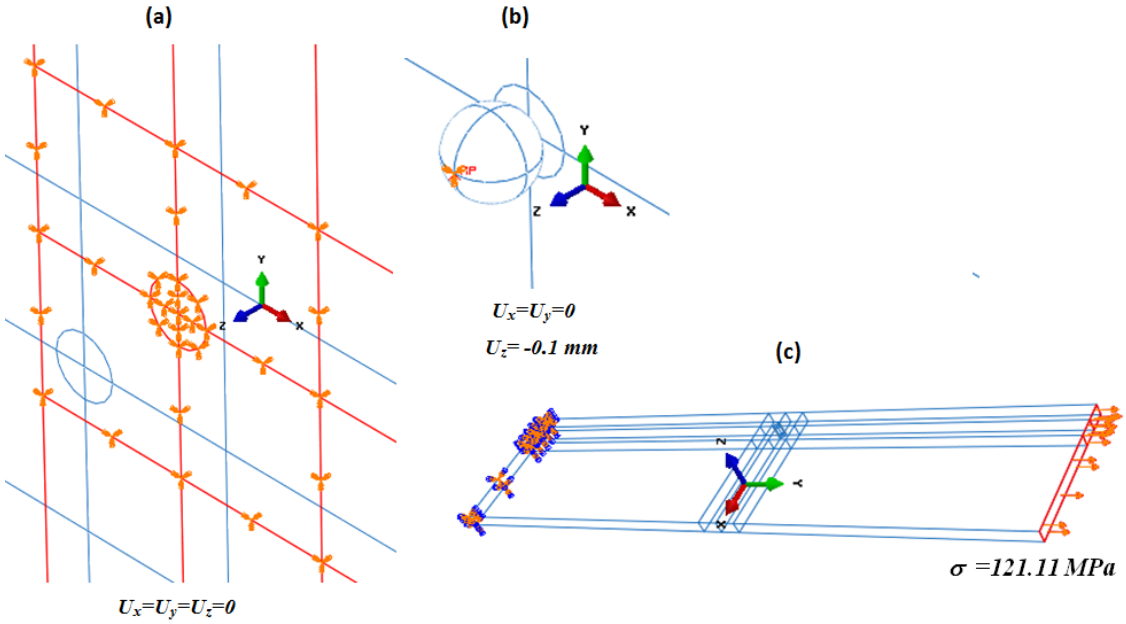

Fig. 4. Boundary Conditions (BC) and Loading, Step 1: (a) BC in the bottom side of the plate; (b) BC imposed to the ball at the reference point and imposed displacement; (c) and Step 2: (d) Clamped edge and tensile loaded edge

J-Integral calculation

With the stress and strain fields calculated around the crack tip, fracture parameter is computed to predict the crack propagation and fatigue life of the indented and non-indented plate in mode I failure. As the material behavior is elastoplastic, the J-integral parameter is used and thus the need for extremely fine meshes near the crack tip in finite element analysis is not needed. The J-integral definition entails evaluating an energy balance for a displacement ahead of the crack along the line propagation. It is characterized as a contour integral that remains path-independent and defined as [28]:

$$J = \oint_{\Gamma} \left[w_{n_1} - \sigma_{ij} n_j \frac{\partial u_i}{\partial x} \right] ds, \tag{1}$$

Here, w, σ_{ij} and u_i denote the strain-energy density, stress components and the displacements along i-axis, respectively. The parameter s denotes the arc length of the contour having n_j component of the unit vector outward normal to the contour Γ. This contour Γ encompasses any path with a vanishing radius surrounding the crack-tip (Fig. 5).

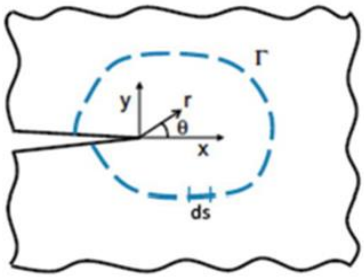

Fig. 5. An arbitrary contour around a crack tip used for the calculation of the J-integral

RESULTS AND DISCUSSION

Residual stresses

The position of the indentation relative to the crack tip (Di) significantly influences the circumferential residual stresses generated by the indentation process. Therefore, indentations were performed at various positions ahead of the crack tip to compare the resulting circumferential residual stresses. Specifically, three positions along the x-axis (the propagation line) were chosen for the indentation process. These positions were defined by the distance from the crack tip, designated as Di = 0 (at the crack tip), Di=0.5, and Di=1 mm. The obtained results are presented in Fig. 6, where the residual stresses along the crack propagation line (x-axis) after indentation are compared.

It is evident from the results that high compressive residual stresses are generated when indentation is performed at the crack tip position (Di=0). Conversely, indentation at a distance of 1 mm away from the crack tip results in tensile compressive stresses, even before any external loading is applied. Indeed, the most critical site is at the crack tip, where stress singularities are anticipated.

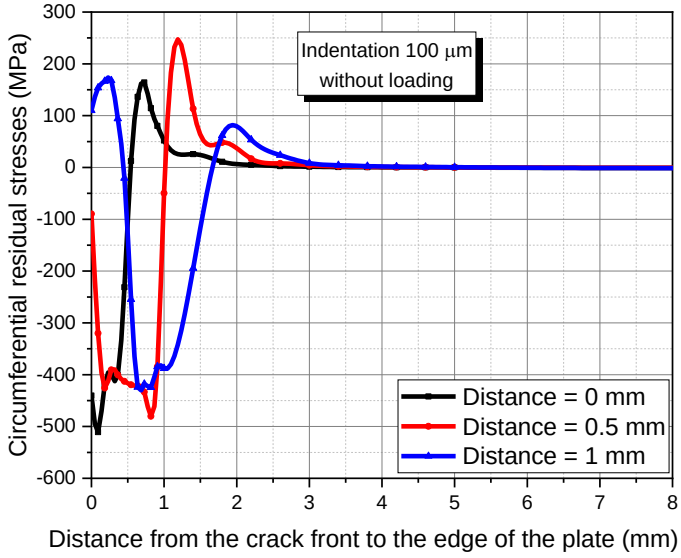

Fig. 6. Comparison between circumferential residual stresses along the distance from the crack tip to the edge of the indented plate

Analyzing the aforementioned figure reveals a consistent pattern across all three positions. Specifically, it is evident that indentation induces compressive residual stresses around the indentation site, which gradually diminish as one moves away. More precisely, the highest compressive stresses are observed for Di = 0 mm position, reaching up to -500 MPa, surpassing those at other positions. Furthermore, a comparison between the 0 mm, 0.5 mm and 1 mm positions indicates that the compressive zone for 1 mm position is notably broader, extending up to 1.6 mm for indentation at Di=1 mm.

For further clarification, Figure 7 depicts the iso-surface of residual stress distribution near the crack tip for the three indentation positions. The stress ranges clearly indicate the presence of compressive residual stresses (depicted by blue surfaces) around the indentation site.

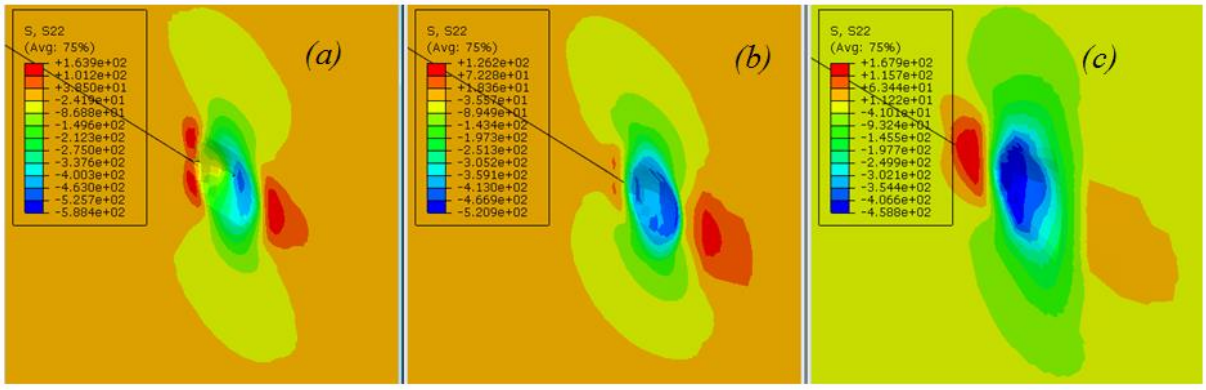

Fig. 7. Distribution of circumferential residual stresses around the crack front of indented plates: a) Di=0; b) Di=0.5, and; c) Di=1 (mm)

Stress evaluation under tensile loading

In this section, we discuss the results obtained after applying a tensile load to the plate. This aspect of the simulation aims to effectively evaluate the influence of the indentation process on the stress field when the plate is under loading conditions.

Figure 8 presents a comparison between stress field values for the three indentation distances. The evolution of stresses before and after loading demonstrates a consistent pattern across all cases. A notable effect is observed in the zone of compressive residual stresses after loading. In all instances, the residual stresses after loading are positive in the vicinity of the crack tip. These findings suggest that the loading absorbs the compressive residual stresses, although these stresses persist in a region ahead of the crack tip with varying magnitudes depending on the indentation distance. This distinction is further emphasized by comparing the stress distributions of reference plate (without indentation) and an indented cracked plate at different distances from the crack tip, as depicted in Figure 9.

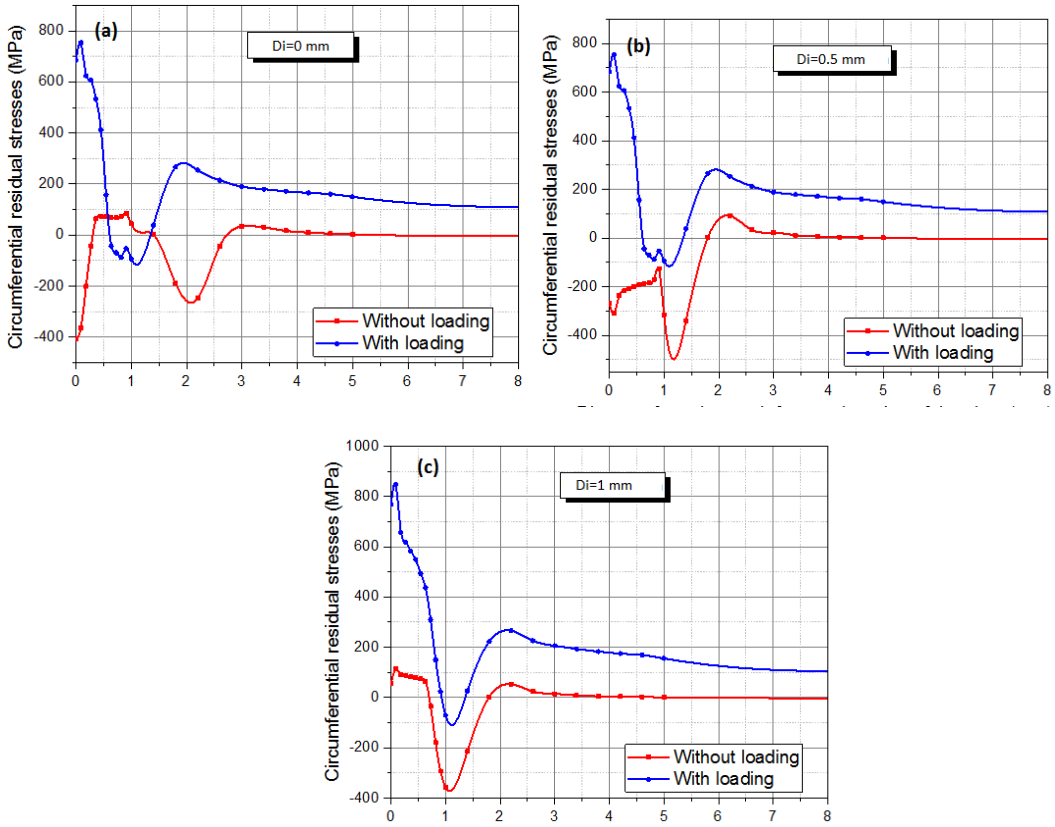

Fig. 8. Comparison of the distribution of circumferential residual stresses before and after tensile loading for DF = a) 0 mm; b) 0.5 mm; and c) 1 mm

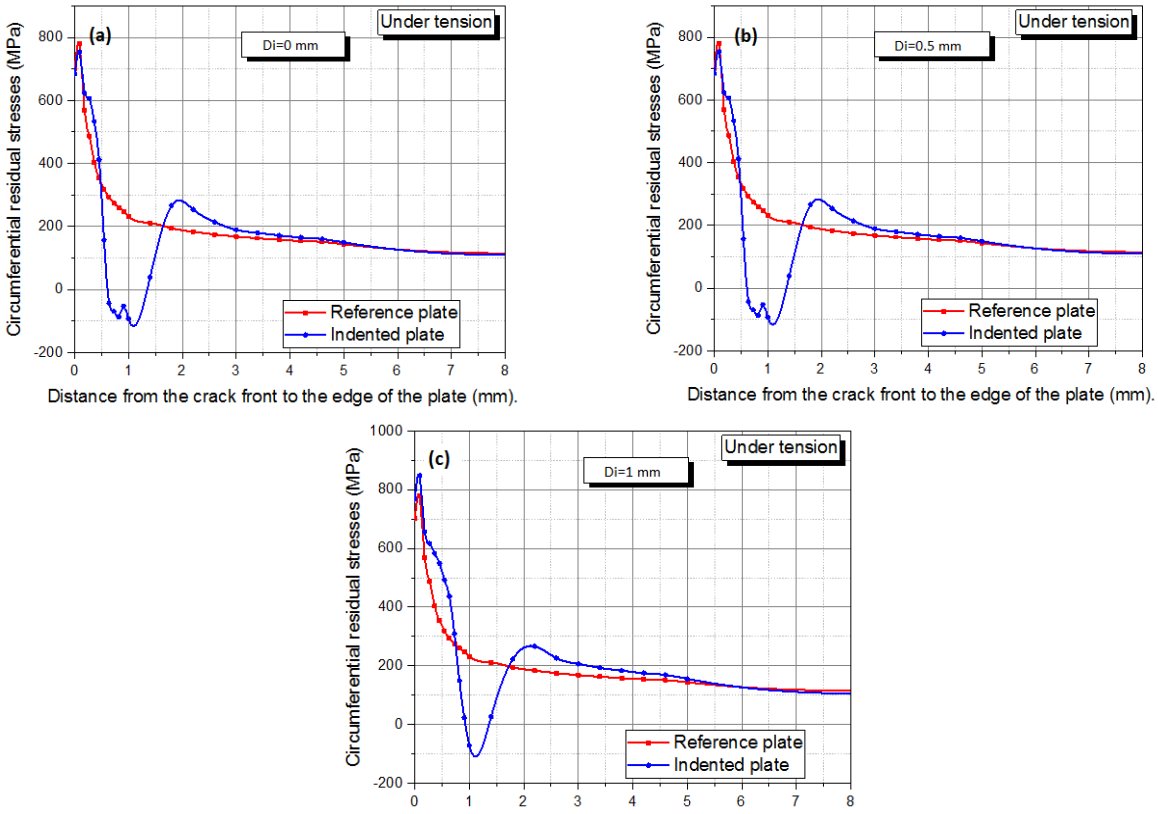

Fig. 9. Comparison of the distribution of residual stresses for reference plate and indented after tensile loading: a) Di=0 mm ; b) Di=0.5 mm ; and c) Di=1 mm

J-integral and crack propagation results

The J-integral is an energy release parameter used to assess the stress intensity at crack locations in cracked components. It quantifies the resistance to crack propagation and predicts the fracture behavior of materials. In this section, the resulted values of the J-integral, as a function of the indentation position is presented to analyze the effect of the indentation respecting different location. This analysis allows us to verify the performance of the indentation in terms of crack propagation resistance and quantify its impact on the structural integrity of materials.

It is clearly observed from Figure 10, that the value of the J-integral varies according to the location of the indentation. Specifically, for the plate indented at a distance of 1 mm, it is noted that the J-integral reaches a maximum value, even exceeding the value obtained for the non-indented cracked plate. This observation suggests that in this case, indentation is disadvantageous as it further increases the stress concentration near the crack tip.

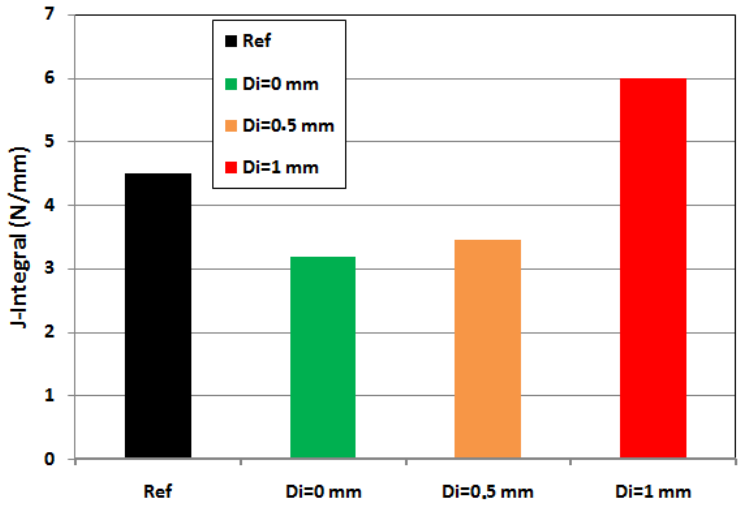

Fig. 10. Comparison of the J-integral values for the different indentation positions and the reference plate

In contrast, for indentations at distances of 0 mm and 0.5 mm from the crack tip, the J-integral values are lower than those for the cracked plate without indentation. Notably, it is observed that indentation directly at the crack tip (Di=0 mm) significantly reduces the J-integral value. This clearly suggests that indentation at this specific location is beneficial, as it reduces stress concentrations around the crack tip.

At this stage of the analysis, it becomes clear that choosing the right indentation location is a key parameter for extending the service life of the cracked plate.

Crack propagation

The J-integral values obtained through the finite element method are converted into stress intensity factors K using the following expression [28]:

$$J = \frac{K_I^2 + K_{II}^2}{E'} + \frac{K_{III}^2}{2\mu} \tag{2}$$

Where KI, KII, and KIII represent the stress intensity factors for mode I (opening), mode II (in-plane shear), and mode III (anti-plane shear), respectively. E' is the effective modulus of

elasticity, and μ is the shear modulus. In the case of plane strain conditions, E' is given by [29]:

$$E' = \frac{E}{1-\nu^2} \tag{3}$$

Since the case studied in this work is in Mode I of failure, expression (2) simplifies to:

$$J = \frac{K_I^2\left(1-\nu^2\right)}{E} \tag{4}$$

Consequently:

$$K = \sqrt{\frac{J.E}{\left(1-\nu^2\right)}} \tag{5}$$

Subsequently, the prediction of fatigue crack growth was carried out using the Forman equation, expressed as follows [13,30]:

$$\frac{da}{dN} = C\left[\left(\frac{1-f}{1-R}\right).\Delta K\right]^m \frac{\left(1-\frac{\Delta K_{th}}{\Delta K}\right)^p}{\left(1-\frac{K_{\max}}{K_c}\right)^q} \tag{6}$$

In this study, we considered a sinusoidal loading cycle with a stress ratio $R = \frac{K_{\min}}{K_{\max}} = 0$, $\Delta K = K_{\max} - K_{\min} = K_{\max}$ and using the fracture parameters provided in Table 3 [28].

Table 3. *Fracture parameters of aluminum 7075-T6 [28,31]*

K_c (MPa.mm$^{0.5}$)	C	m	p	q	f	ΔK_{th} (MPa.mm$^{0.5}$)
1050	3.6×10^{-11}	3.282	0.5	1	0.39584	101.5

Thus, crack propagation per loading cycle da/dN is obtained for the non-indented cracked plate and the various indentation positions. Figure 11 illustrates the obtained results where, a comparison between the different cases is presented.

To highlight the effect of indentation on the crack growth rate, it is advisable to calculate the crack growth gain relatively to crack growth rate of reference cracked plate using the following equation:

$$RG = \frac{da/dN_{Di} - da/dN_{ref}}{da/dN_{ref}} \times 100 \tag{7}$$

Where, da/dN_{Di} represents the crack propagation rate for indented plate Di=0, 0.5 and 1 mm, and da/dN_{ref} represents the crack propagation rate for the reference cracked plate (without indentation).

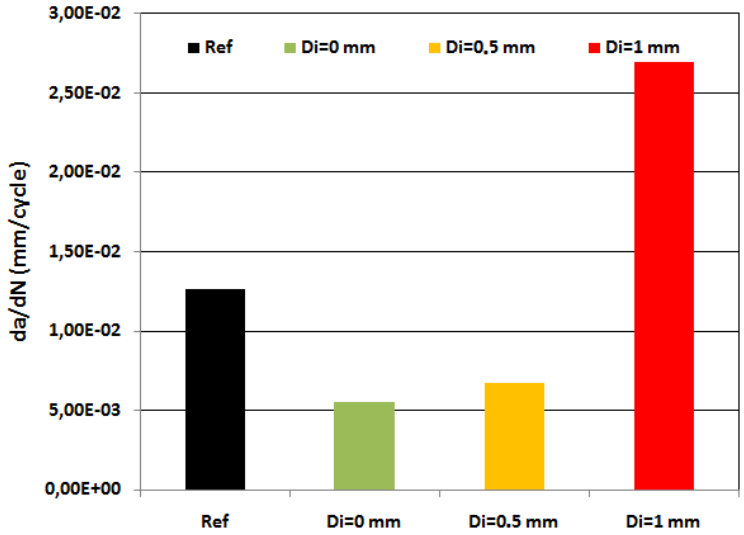

Fig. 11. Comparison of crack propagation for different indentation position and reference non-indented crack

As expected, indentation at the distance Di=0 mm significantly reduces the crack growth rate per loading cycle. Indeed, a relative gain in propagation rate of 56.14% was achieved compared to the non-indented cracked plate (Fig.12). It is also observed that indentation at Di=0.5 mm results in a relative propagation rate gain of 46.62%. Conversely, indentation at Di=1 mm led to a loss in crack propagation rate of -102.59%. Thus, these results confirm that indentation with a spherical ball has a positive effect on delaying crack propagation if performed in the immediate vicinity of the crack tip. Specifically, indentation at the crack tip yields the maximum positive effect.

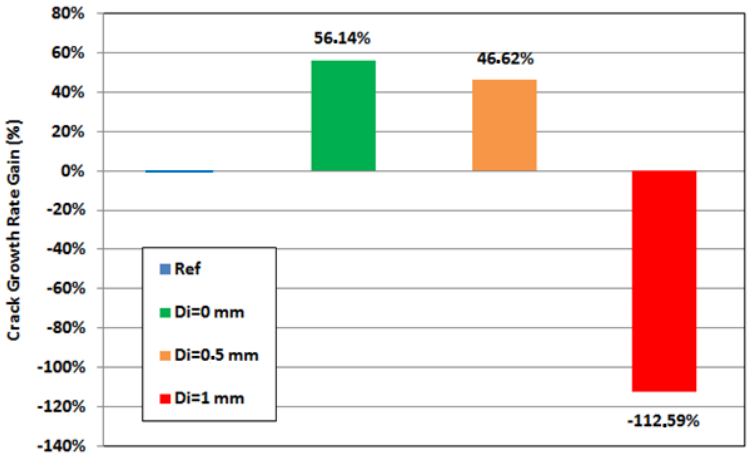

Fig. 12. Crack growth rate gain comparison between reference cracked plate and different position indented plate

CONCLUSIONS

This study addressed the fracture behavior of cracked structures, aiming to extend their lifespan through an indentation technique using the finite element method in Abaqus 6.14. An examination of residual stresses induced by indentation around the crack tip without tensile

loading was done and how this indentation affects the resulted residual stresses under uniaxial tensile loading conditions. Subsequently, the J-integral was calculated to evaluate the indentation's effectiveness in delaying crack propagation. The principal conclusions are summarized as follows:

- Indentation generates residual stresses near the crack tip, the magnitude of which varies depending on the position of indentation.
- Indentation performed ahead of the crack tip (Di=1mm) resulted in tensile residual stresses surrounding the crack tip, while indentation closer to the crack tip (at the crack tip and at 0.5 mm ahead) led to compressive residual stresses.
- Particularly, indentation at position Di=0 mm (at the crack tip) produced the most favorable effect due to the highest compressive residual stress it generated.
- Upon loading, there was a notable absorption of compressive residual stresses, irrespective of the indentation position, resulting in positive stresses.
- The variation in J-integral values is influenced by the indentation position.
- Indentation at a distance of 1 mm from the crack tip yielded higher J-integral values, indicating maximum stress intensity. This suggests an inappropriate choice of indentation position, corroborated by a higher crack propagation rate.
- Conversely, for indentations at the crack tip position (Di=0 mm), minimal J-integral values were observed, suggesting that indentation in this position is desirable.
- The results demonstrate that indentation at the crack tip effectively delays crack propagation, with up to a 56.12% reduction in crack growth rate per loading cycle. However, indentation performed away from the crack (1 mm ahead) accelerates crack propagation and consequently compromises the integrity of the cracked component.

Conflicts of Interest

The authors declare that they have no competing financial interests or personal relationships that could have seem to influence the study reported in this paper.

REFFERENCES

1. S.M. Walley, Historical origins of indentation hardness testing, Mater. Sci. Technol. (United Kingdom). 28 (2012) 1028–1044. https://doi.org/10.1179/1743284711Y.0000000127.
2. S. Arunkumar, A Review of Indentation Theory, Mater. Today Proc. 5 (2018) 23664–23673. https://doi.org/10.1016/j.matpr.2018.10.156.
3. G.D. Quinn, R.C. Bradt, On the Vickers Indentation Fracture Toughness Test, 680 (2007) 673–680. https://doi.org/10.1111/j.1551-2916.2006.01482.x.
4. N. Ogasawara, N. Chiba, X. Chen, Measuring the plastic properties of bulk materials by single indentation test, 54 (2006) 65–70. https://doi.org/10.1016/j.scriptamat.2005.09.009.
5. J. Hay, Introduction to instrumented indentation testing, Exp. Tech. 33 (2009) 66–72.
6. T. Nakamura, T. Wang, S. Sampath, Determination of properties of graded materials by inverse analysis and instrumented indentation, Acta Mater. 48 (2000) 4293–4306. https://doi.org/10.1016/S1359-6454(00)00217-2.
7. H. Wang, L. Zhu, B. Xu, Residual Stresses and Nanoindentation Testing of Films and Coatings, Residual Stress. Nanoindentation Test. Film. Coatings. (2018) 21–36. https://doi.org/10.1007/978-981-10-7841-5.

8. J. Fu, S. Kamali-Bernard, F. Bernard, M. Cornen, Comparison of mechanical properties of C-S-H and portlandite between nano-indentation experiments and a modeling approach using various simulation techniques, Compos. Part B Eng. 151 (2018) 127–138. https://doi.org/10.1016/j.compositesb.2018.05.043.
9. A. Alhasanyah, T.K. Vaidyanathan, R.J. Flinton, Effect of core thickness differences on post-fatigue indentation fracture resistance of veneered zirconia crowns, J. Prosthodont. 22 (2013) 383–390. https://doi.org/10.1111/jopr.12016.
10. W.K. Lim, J.H. Song, B. V. Sankar, Effect of ring indentation on fatigue crack growth in an aluminum plate, Int. J. Fatigue. 25 (2003) 1271–1277. https://doi.org/10.1016/j.ijfatigue.2003.08.011.
11. T.W. Clyne, J.E. Campbell, M. Burley, J. Dean, Profilometry-Based Inverse Finite Element Method Indentation Plastometry, Adv. Eng. Mater. 23 (2021). https://doi.org/10.1002/adem.202100437.
12. N. Razavi, M.R. Ayatollahi, A. Amouzadi, F. Berto, Effects of different indentation methods on fatigue life extension of cracked specimens, Fatigue Fract. Eng. Mater. Struct. 41 (2018) 287–299. https://doi.org/10.1111/ffe.12678.
13. R. Růžek, J. Pavlas, R. Doubrava, Application of indentation as a retardation mechanism for fatigue crack growth, Int. J. Fatigue. 37 (2012) 92–99. https://doi.org/10.1016/j.ijfatigue.2011.09.012.
14. X.D. Hou, N.M. Jennett, A method to separate and quantify the effects of indentation size, residual stress and plastic damage when mapping properties using instrumented indentation, J. Phys. D. Appl. Phys. 50 (2017). https://doi.org/10.1088/1361-6463/aa8a22.
15. S. Syngellakis, H. Habbab, B.G. Mellor, Finite element simulation of spherical indentation experiments, Comput. Exp. Stud. (2018) 129.
16. M. Aldarwish, A. Grbović, G. Kastratović, A. Sedmak, M. Lazić, Stress intensity factors evaluation at tips of multi-site cracks in unstiffened 2024-t3 aluminium panel using XFEM, Teh. Vjesn. 25 (2018) 1616–1622. https://doi.org/10.17559/TV-20170309133824.
17. Y.A. Fageehi, A.M. Alshoaibi, Nonplanar Crack Growth Simulation of Multiple Cracks Using Finite Element Method, Adv. Mater. Sci. Eng. 2020 (2020). https://doi.org/10.1155/2020/8379695.
18. B. Seyfi, N. Fatouraee, M. Imeni, Mechanical modeling and characterization of meniscus tissue using flat punch indentation and inverse finite element method, J. Mech. Behav. Biomed. Mater. 77 (2018) 337–346. https://doi.org/10.1016/j.jmbbm.2017.09.023.
19. S. Carlsson, P.-L. Larsson, On the determination of residual stress and strain fields by sharp indentation testing.: Part II: experimental investigation, Acta Mater. 49 (2001) 2193–2203.
20. N. Huber, J. Heerens, On the effect of a general residual stress state on indentation and hardness testing, Acta Mater. 56 (2008) 6205–6213.
21. N. Razavi, M.R. Ayatollahi, F. Berto, Assessment of fatigue crack growth behavior of cracked specimens repaired by indentation, Procedia Struct. Integr. 13 (2018) 69–73.
22. L. Deng, J. Zhao, Z. Wang, Estimation of residual stress of metal material with yield plateau by continuous spherical indentation method, Mater. Res. Express. 7 (2020). https://doi.org/10.1088/2053-1591/ab7069.
23. P. Chantikul, G.R. Anstis, B.R. Lawn, D.B. Marshall, A critical evaluation of indentation techniques for measuring fracture toughness: II, strength method, J. Am. Ceram. Soc. 64 (1981) 539–543.
24. N.H. Faisal, R. Ahmed, R.L. Reuben, Indentation testing and its acoustic emission response:

applications and emerging trends, Int. Mater. Rev. 56 (2011) 98–142.

25. T.N. Chakherlou, J. Vogwell, The effect of cold expansion on improving the fatigue life of fastener holes, Eng. Fail. Anal. 10 (2003) 13–24.
26. A. Djebli, A. Baltach, M. Lallam, M. Bendouba, Numerical Analysis of Plate Thickness Effect on Residual Stress Distribution around a Cold Expanded Hole, Trans. FAMENA. 47 (2023) 47–59.
27. A. Baltach, A. Djebli, M. Bendouba, A. Aid, others, Numerical analysis and optimization of the residual stresses distribution induced by cold expansion technique, Frat. Ed Integrità Strutt. 12 (2018) 252–265.
28. H. Hosseini-Toudeshky, B. Mohammadi, H.R. Daghyani, Mixed-mode fracture analysis of aluminium repaired panels using composite patches, Compos. Sci. Technol. 66 (2006) 188–198.
29. M. Bendouba, A. Djebli, A. Aid, N. Benseddiq, M. Benguediab, Time-dependent J-integral solution for semi-elliptical surface crack in HDPE, C. Mater. Con. 45 (2015) 163–186.
30. Harter JA. AFGROW users guide and technical manual, AFRL-VA-WP-TR-2008, Air Force Research Laboratory, Ohio, USA; 2008
31. B. Farahmand, G. Bockrath, J. Glassco, Fatigue and fracture mechanics of high risk parts: application of LEFM \& FMDM theory, Springer Science \& Business Media, 2012.